

Effective Interaction Potentials for Alkali and Alkaline Earth Metal Ions in SPC/E Water and Polarization Model of Hydrated Ions

Sergei Gavryushov*

Engelhardt Institute of Molecular Biology, 32 Vavilova St., Moscow, Russia

Received: November 27, 2005; In Final Form: April 14, 2006

In the first paper (*J. Phys. Chem. B*, 2006, 110, 10878), effective ion–ion potentials in SPC/E water were obtained for Me–Me, Me–Cl[−], and Cl[−]–Cl[−] pairs, where Me is Li⁺, Na⁺, K⁺, Mg²⁺, Ca²⁺, Sr²⁺, and Ba²⁺ cations. In this second part of the study of effective interionic potentials, ion–ion distribution functions obtained from implicit-water Monte Carlo simulations of electrolyte solution with these potentials have been explored. This analysis verifies the range of applicability of the primitive model of electrolyte. It is shown that this approximation can be applied to monovalent electrolyte solutions in a wide range of concentrations, whereas the nature of ion–ion interactions is notably different for 2:1 electrolytes. An improved model of ions is discussed. The model includes approximations of the ion hydration shell polarization and specific short-range ion–ion interaction. It allows approximation of the potential of mean force acting on ions in strong electric fields of highly charged macromolecules and bilayers.

Introduction

In the first part of this study,¹ further called paper 1, potentials of mean force (PMF) between two hydrated ions at infinity dilution (or effective interionic potentials) have been obtained from molecular dynamics (MD) simulations for Me–Me, Me–Cl[−], and Cl[−]–Cl[−] interactions. Here Me denotes Li⁺, Na⁺, K⁺, Mg²⁺, Ca²⁺, Sr²⁺, and Ba²⁺ cations. A rigid SPC/E model of water² was applied. Those effective potentials were used in implicit-solvent Monte Carlo (MC) simulations of electrolyte solutions to compare the simulated mean activity coefficients of electrolytes with experimental data at concentrations of 0.1–1 M.

It was shown that predictions of NaCl and KCl activity coefficients were successful for some Lennard–Jones (LJ) approximations of ion–water interactions,^{3–5} whereas for other LJ potentials³ of KCl, they were not. In the case of LJ approximations for the lithium cation,^{3,6} the obtained activities are rather lower than the observed ones, which may indicate either an incorrect LJ approximation or a wrong application of the SPC/E water model to LJ parameters derived from a polarizable model of water.⁶ In the case of LJ parameters for alkaline earth metal ions,³ the effective interionic potentials lead to simulated activity coefficients, which agree with experimental data only at $c < 0.1$ M. This indicates the importance of three-body interactions and ion hydration shell polarization deficiency effects at higher concentrations of 2:1 electrolyte.

The effective interionic potentials allow us to verify simplifications of the primitive model (PM) of hydrated ions. The model represents a hypothetical electrolyte, where ions are hard spheres dissolved in structureless solvent described by the dielectric constant. It has been widely applied to explore the finite ion size and interionic correlation effects in the theory of electrolyte solution and double layers. To account for these effects, the integral equations,^{7–10} modified Poisson–Boltzmann (MPB) theory,¹¹ and cluster expansion theory^{12,13} were used.

All these approaches demonstrated importance of the finite ion size effects and interionic correlation effects even at moderate concentrations of electrolyte. It was shown that experimental activity coefficients of 1:1 electrolyte could be reproduced by PM calculations when the ion hard-core radii were adjusted to realistic values.¹⁰ The finite ion size effects of the PM were incorporated into an exact statistical mechanical formalism of the dressed ion theory.¹⁴ On the basis of the density functional analysis, the corrected Debye–Hückel (DH) theory was developed.^{15,16} Finally, the PM has been used in MC simulations^{17–19} to verify the integral equation, cluster expansion, and MPB theories.

As seen from, e.g., ref 20 or Figures 4–5 and 9–10 of paper 1, the solvent-mediated ion–ion PMFs notably differ from the hard-core repulsion at close contact of ions. One of the objectives of the present work is a verification of the role of hard-core interactions and interionic correlations in the thermodynamics of electrolyte solutions. To distinguish between the two effects, the effective interionic potentials from paper 1 were incorporated into statistical mechanical equations to calculate the ion activity coefficients for dilute electrolyte solution. It gives a mean-field approximation for the ion activity coefficient. As those effective potentials were used in MC simulations of electrolyte solutions reported in paper 1, the role of interionic correlations can be seen from a difference of the ion chemical potentials obtained by the MC simulations and by the mean-field calculations. In the present work, such an analysis is done for NaCl, KCl, MgCl₂, and CaCl₂.

Another issue is a polarization deficiency of the ion hydration shell due to dielectric saturation. This effect leads to the law for the permittivity of the solution:

$$\epsilon(c) = \epsilon - \sum \delta_i c_i \quad (1)$$

Here, c_i is the concentration of ions of species i , δ_i a positive ion-specific coefficient, and ϵ the permittivity of pure water. The polarization energy of the ion hydration shell is $\alpha_i E^2$, where E is the external electric field intensity and α_i is connected to

* Corresponding author. E-mail: sergei_gavryushov@yahoo.com.

the experimental value of δ_i by the relationship (SI units)²¹

$$\alpha_i = \frac{1}{1000N_A} \frac{\epsilon_0}{2} \delta_i \quad (2)$$

Equation 1 has been discussed since Hückel's work²² and confirmed by measurement²³ and computer simulations.^{21,24,25} A need to take this effect in electrolyte theory was discussed in recent works.²⁶ As shown in paper 1, comparison of MC-simulated activities with experimental data suggests that the ion hydration shell polarization effects might be important in the case of 2:1 electrolytes. So, including eq 1 into calculation of thermodynamic quantities of electrolyte is also discussed in the present work.

Finally, an improvement of the primitive model of ions will be discussed. Such an approximate model can be applied in MC simulations or MPB calculations of double layers near highly charged macromolecules and bilayers. The inclusion of the ion hydration shell polarization into a simplified model of hard-core interacting ions was already discussed in ref 21 and named the primitive polarization model (PPM). The effective interionic potentials reported in paper 1 allow further development of this model. Now it can include an approximation of the specific short-range interionic interactions.

Mean-Field Approximation of Ion–Ion Interaction²⁷

In this section, effective ion–ion potentials shown in Figures 4–5 and 9–10 of paper 1 will be applied to calculate the ion chemical potential for dilute solutions. Results will be compared with ion activity coefficients obtained from MC simulations with the same effective interionic potentials. This comparison will be made for NaCl, KCl, MgCl₂, and CaCl₂ potentials. It will allow us to verify the role of interionic correlations and ion hydration shell polarization deficiency in systems with solvent-mediated potentials.

Activity Coefficient of Dilute Electrolyte. The effective ion–ion potential at infinity dilution can be written as a sum of the short-range and Coulomb parts:

$$u_{ij}^0(r) = u_{ij}^{\text{SR}}(r) + Z_i Z_j e^2 / (\epsilon r) \quad (3)$$

where $u_{ij}^{\text{SR}}(r)$ in general includes ion hydration shell polarization energy ($\alpha_i E_j^2 + \alpha_j E_i^2$) at long distances between ions, Z_i is the ion valence, e the elementary charge, and ϵ the permittivity of water. These two terms of the interionic PMF will be retained at a finite concentration of ions. At low ionic concentrations, ions are mainly pairs interacting at short distances, therefore, the short-range part u^{SR} will not be much affected, and the ion–ion PMF at finite ionic concentration can be written as

$$u_{ij}(r) \approx u_{ij}^{\text{SR}}(r) + Z_j e \psi_i(r) \quad (4)$$

Here $\psi_i(r)$ is the mean electrostatic potential around the fixed ion i . It can be easily shown that, at large r (where the short-range potential vanishes),

$$\psi_i(r) = C_i \exp(-\kappa r) / r \quad (5a)$$

where C_i is a constant, and κ the inverse DH length. On the other hand, eq 4 can also be written as $u_{ij}(r) \approx u_{ij}^{\text{SR}}(r) + Z_i e \psi_j(r)$, where $\psi_j(r)$ satisfies the same dependence on r :

$$\psi_j(r) = C_j \exp(-\kappa r) / r \quad (5b)$$

where C_j is another constant. By combining eqs 5a and b, one

obtains the equation

$$u_{ij}(r) \approx u_{ij}^{\text{SR}}(r) + Z_i Z_j e^2 C_{ij} \exp(-\kappa r) / r \quad (6)$$

where $C_{ij} = (C_i/Z_i + C_j/Z_j)/2e$.

It follows from the theory and also from simulated ion–ion radial distribution functions (RDFs) that, at dilution of PM electrolyte, the $Z_i Z_j e^2 C_{ij} \exp(-\kappa r) / r$ term becomes the well-known exponential form of the DH theory:

$$u_{ij}^{\text{DH}}(r) = \frac{Z_i Z_j e^2}{\epsilon(1 + \kappa a)} \frac{\exp(-\kappa(r - a))}{r} \quad (7)$$

where a is the hard-core diameter of PM ions.

When the short-range part of the pair potential is different from the hard-sphere repulsion, one can introduce an adjustable parameter a to write eq 6 in the form (eq 7). At low ionic concentrations and large Debye–Hückel lengths ($\kappa < 0.1$ M, $\lambda_{\text{DH}} = 1/\kappa > \sim 10$ Å), it is just formal expression of the C_{ij} constant in eq 6.

After substitution of eq 7, eq 6 will be written as

$$u_{ij}(r) = u_{ij}^{\text{SR}}(r) + u_{ij}^{\text{DH}}(r) \quad (8)$$

where u_{ij}^{SR} is the short-range part of the effective ion–ion potential, and u_{ij}^{DH} the mean field potential averaging the long-range electrostatics and written like the Debye–Hückel potential. In its expression, we have introduced the new parameter a_{ij} as an “effective” diameter for interaction of ions of species i and j :

$$u_{ij}(r) \approx u_{ij}^{\text{SR}}(r) + \frac{Z_i Z_j e^2}{\epsilon(1 + \kappa a_{ij})} \frac{\exp(-\kappa(r - a_{ij}))}{r} \quad (9)$$

$r > a_{ij}$.

At $r < a_{ij}$, the screening effects of the mean electric field can be neglected, and it may be assumed that the mean electrostatic potential is just the Coulomb potential shifted by a constant to the $u_{ij}^{\text{DH}}(a_{ij})$. The value of a_{ij} is extracted from the constant C_{ij} in eq 6 according to eq 9. The constant C_{ij} is obtained from fitting the asymptotes of ion–ion PMFs to expression 6 at large ion–ion separation r where $u_{ij}^{\text{SR}}(r)$ vanishes. The PMFs themselves are extracted from ion–ion RDFs obtained by MC simulations of electrolyte solution with effective ion–ion potentials.

One can also express C_{ij} in eq 6 using different adjustable parameters. For example, a common size a of all ions and their “dressed” charges Z_i^* and Z_j^* can be introduced instead of a_{ij} :

$$u_{ij}(r) \approx u_{ij}^{\text{SR}}(r) + \frac{Z_i^* Z_j^* e^2}{\epsilon(1 + \kappa a)} \frac{\exp(-\kappa(r - a))}{r}$$

In the following, eq 9 will be used.

The activity coefficient, γ_i , of species i can be given by the equation²⁸

$$\ln \gamma_i = \sum_k n_k^0 \int d\mathbf{r}_j \beta u_{ik}^0(\mathbf{r}_{12}) \int_0^1 g_{ik}(\mathbf{r}_{12}, \lambda) d\lambda \quad (10)$$

where $\beta = 1/kT$, n_k^0 is the bulk particle density of species k , g_{ik} the radial distribution function, and the pair potential u_{ik}^0 is multiplied by the coupling parameter λ whenever particle 1 of species i appears. By taking into account eqs 9 and 10, the

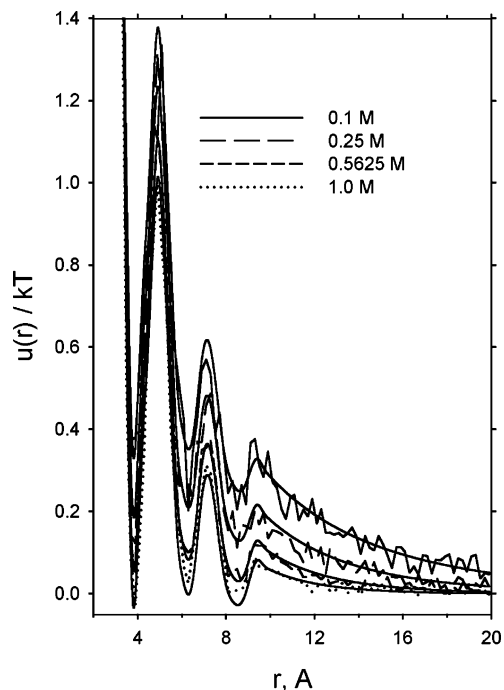


Figure 1. $\text{Na}^+ - \text{Na}^+$ PMFs obtained from MC simulations of NaCl solutions at electrolyte concentrations of 0.1, 0.25, 0.5625, and 1.0 M. Smooth curves are calculated via eq 9 with a short-range effective potential of $\text{Na}^+ - \text{Na}^+$ (ion LJ parameters from refs 4 and 5). Parameter a_{NaNa} is set to 5.5 Å at all four concentrations.

excess chemical potential of an ion of species i can be expressed as

$$\mu_i = \sum_j 4\pi n_j^0 \int_0^\infty dr r^2 \left(u_{ij}^{\text{SR}}(r) + \frac{q_i q_j}{\epsilon r} \right) \times \int_0^1 d\lambda \exp(-\beta \lambda (u_{ij}^{\text{SR}}(r) + q_i \psi_{ij}(r))) \quad (11)$$

where

$$\psi_{ij}(r) = \begin{cases} \frac{q_i}{\epsilon(1 + \kappa a_{ij})} \frac{\exp(-\kappa(r - a_{ij}))}{r}, & r > a_{ij} \\ \frac{q_i}{\epsilon r} + V_{ij}, & r < a_{ij}, \end{cases} \quad V_{ij} = -\frac{q_i \kappa}{\epsilon(1 + \kappa a_{ij})}$$

Expression 11 is correct at neglecting an induced polarization component in u_{ij}^{SR} . This part of u_{ij}^{SR} would be proportional to λ^2 .

Monovalent Electrolytes. In the case of 1:1 electrolyte, it was found that approximation 9 was good not only at $c \sim 0.1$ M but also at a concentration up to 1 M. In Figures 1–3, comparisons of NaCl PMFs with approximation 9 are shown at different ionic concentrations. The simulated PMFs were derived from RDFs obtained by MC simulations with effective potential (eq 3) and u_{ij}^{SR} shown in Figures 4–5 of paper 1. One can see that eq 9 not only fits PMFs with an excellent accuracy, but the adjusted parameter a_{ij} is rather ion-specific and weakly depends on ionic concentration. The effective diameter of Na^+ appears to be of 5.5 Å, and the effective diameter of Cl^- is from 4 to 4.5 Å. Values of a_{ij} for NaCl and KCl are collected in Table 1.

To evaluate the accuracy of eq 11, this expression was integrated with respect to λ and calculated numerically by using spline interpolations of the potentials u_{ij}^{SR} . In Figure 4, mean

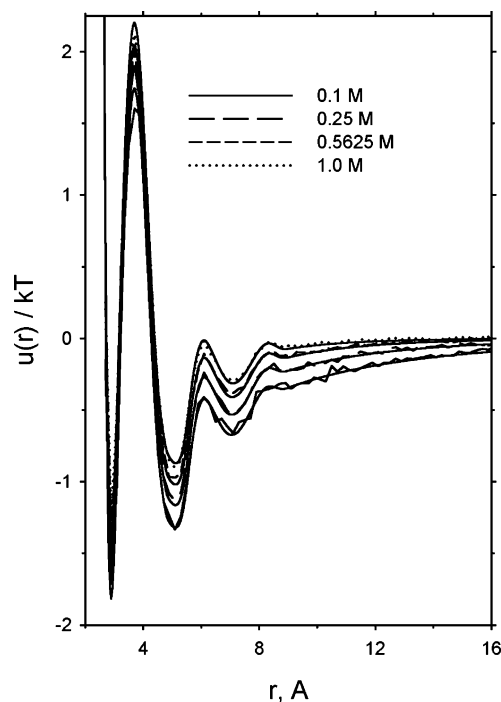


Figure 2. $\text{Na}^+ - \text{Cl}^-$ PMFs obtained from MC simulations of NaCl solutions at electrolyte concentrations of 0.1, 0.25, 0.5625, and 1.0 M. Smooth curves are calculated via eq 9 with a short-range effective potential of $\text{Na}^+ - \text{Cl}^-$ (ion LJ parameters from refs 4 and 5). Parameter a_{NaCl} is set to 5 Å at concentrations of 0.1, 0.25, and 0.5625 M, and to 4.5 Å at $c = 1$ M.

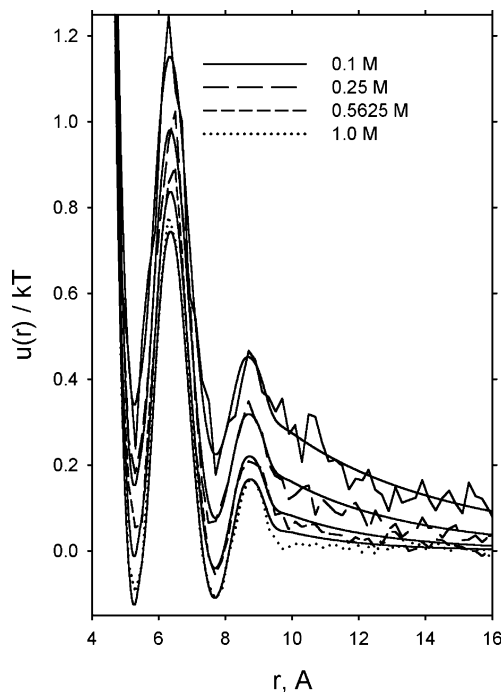


Figure 3. $\text{Cl}^- - \text{Cl}^-$ PMFs obtained from MC simulations of NaCl solutions at electrolyte concentrations of 0.1, 0.25, 0.5625, and 1.0 M. Smooth curves are calculated via eq 9 with a short-range effective potential of $\text{Cl}^- - \text{Cl}^-$ (ion LJ parameters from refs 4 and 5). Parameter a_{ClCl} is set to 4.5 Å at $c = 0.1$ M and to 4 Å at higher concentrations of ions.

activity coefficients of NaCl and KCl calculated via eq 11 are compared with results of MC simulations from paper 1 and with experimental data.²⁹ The potentials u_{ij}^{SR} used are shown in Figures 4–5 of paper 1 (LJ parameters^{4,5} of Cl^- , Na^+ , and K^+). Effective sizes a_{ij} are given in Table 1. The crucial point is a

TABLE 1: Ion Interaction Parameters from Effective Ion–Ion Potentials and Ion–Ion Distribution Functions

electrolyte	ij^a	a_{ij} (Å)	a_{ij}^{HC} (Å)
NaCl	11	5.5	3.2
	12	4.5	2.7
	22	4.0	4.3
KCl	11	5.5	3.8
	12	3.5	2.8
	22	4.0	4.3
MgCl ₂	11	7.0	6.0
	12	5.5	3.7
	22	3.5	4.3
CaCl ₂	11	6.0	6.0
	12	4.7	3.9
	22	2.0	4.3

^a For electrolyte MeCl or MeCl₂, Me⁺ or Me²⁺ –1, Cl[–] –2.

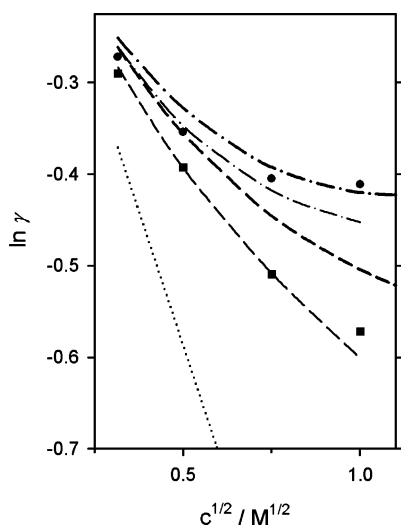


Figure 4. NaCl and KCl activity coefficient calculations based on the effective ion–ion potentials reported in paper 1. Filled circles and squares are results of MC simulations of solutions of NaCl and KCl, respectively. The thin dash–dotted and dashed curves are activity coefficients calculated via eq 11 for NaCl and KCl, respectively. The thick dash–dotted curve represents experimental data for NaCl. The thick dashed curve is experimental data for KCl. The dotted line is the DH limiting law.

comparison of results obtained via eq 11 with results of MC simulations. As seen from Figure 4, the agreement between them is observed up to 0.6 M concentration of 1:1 electrolyte. The successful reproduction of the MC-simulated activity coefficients of 1:1 electrolytes by mean-field approximation (eq 9) with constant parameters a_{ij} suggests that the interionic correlations play only a minor role in such systems. At a concentration of 1 M, some deviation is observed, which might suggest an appearance of the interionic correlation effects. On the other hand, as discussed in paper 1, errors in MD-simulated potentials u_{ij}^{SR} lead to statistical uncertainty in the MC-simulated $\ln \gamma$ of about 0.05 at $c = 1$ M, which is higher than this deviation. Therefore, the disagreement between eq 11 and MC simulations does not exceed model errors at all concentrations studied.

The activity coefficient deviations due to polarization effects (eq 1) do not exceed model errors either. For 1:1 electrolytes, such a deviation of $\ln \gamma$ is negligible at $c = 0.1$ M and it can reach 0.1 at $c = 1$ M (paper 1). As follows from a comparison of MC-simulated and experimental activity coefficients shown in Figure 4, model errors originating from inaccuracy of the LJ approximation are much higher at $c = 0.1$ M, and they are of the same magnitude of 0.1 at $c = 1$ M. As a result, we may

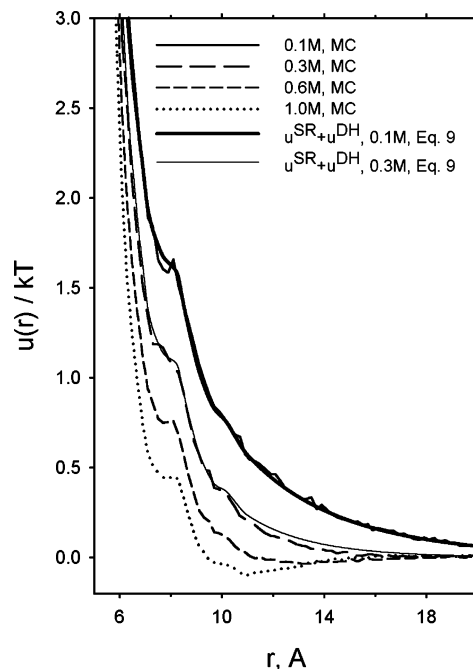


Figure 5. Mg^{2+} – Mg^{2+} PMFs obtained from MC simulations of MgCl_2 solutions at electrolyte concentrations of 0.1, 0.3, 0.6, and 1.0 M. Two smooth curves are calculated via eq 9 with a short-range effective potential of Mg^{2+} – Mg^{2+} (LJ parameters of Mg^{2+} from ref 3). Parameter a_{MgMg} is set to 7.2 and 7.0 Å at concentrations of 0.1 and 0.3 M, respectively. At concentrations of 0.6 and 1.0 M, overneutralization is observed, and the coefficient C from eq 6 becomes negative.

also disregard the polarization effects in the case of 1:1 electrolyte solutions.

Divalent Cations. A similar analysis as done for NaCl and KCl was applied to MgCl_2 and CaCl_2 . First, approximation 9 was tested on the results of implicit-water MC simulations with the effective interaction potentials for divalent cations and Cl^- . As for 1:1 electrolyte, there were used the effective ion–ion potentials presented in paper 1. Details of the MC simulations are described in paper 1.

Comparisons of eq 9 with MC simulations for MgCl_2 are shown in Figures 5–7. The Mg^{2+} – Mg^{2+} , Mg^{2+} – Cl^- , and Cl^- – Cl^- PMFs are chosen at electrolyte concentrations of 0.1, 0.3, 0.6, and 1 M, respectively. At $c = 0.6$ and 1 M, overneutralization of both Mg^{2+} and Cl^- ions is observed, but at lower concentrations, the simulated pair distributions satisfy eq 9 at $a_{\text{MgMg}} = 7.2$ Å, $a_{\text{MgCl}} = 5.5$ Å, and $a_{\text{ClCl}} = 3.5$ Å. A similar analysis was applied to results of MC simulations for CaCl_2 . Values of the ion effective sizes a_{ij} for MgCl_2 and CaCl_2 are collected in Table 1.

As seen from Figures 5–6, at $c = 0.6$ and 1 M, the asymptotic behavior of interionic PMFs requires negative factor C_{ij} in eq 6, which cannot be satisfied by eq 9 in principle. For example, $u_{\text{MgMg}}(r|c = 1 \text{ M})$ becomes negative at $r > 9.5$ Å, and $u_{\text{MgMg}}(r|c = 0.6 \text{ M})$ is negative at $r > 11$ Å (Figure 5). It means that mean-field approximation (eq 9) does not endure when the concentration of 2:1 electrolyte increases. Overneutralization is also observed for all RDFs (i.e. Me^{2+} – Me^{2+} , Me^{2+} – Cl^- , and Cl^- – Cl^-) obtained for divalent cations of Mg, Ca, Sr, and Ba at $c = 0.6$ and 1 M. So, the interionic correlations play an important role for long-range electrostatic interactions in such systems.

Anyway, the successful approximation of the ion–ion PMFs by eq 9 at $c < 0.3$ M allows us to apply eq 11 to 2:1 electrolyte solutions at least at $c < 0.3$ M. Activity coefficients calculated via eq 11 are shown in Figure 8. One can see that this

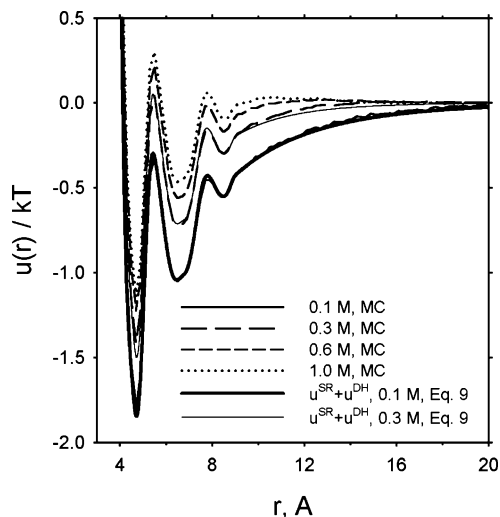


Figure 6. Mg^{2+} – Cl^- PMFs obtained from MC simulations of MgCl_2 solutions at electrolyte concentrations of 0.1, 0.3, 0.6, and 1.0 M. Notations as in Figure 5. Parameter a_{MgCl} is set to 5.5 Å at concentrations of 0.1 and 0.3 M. At concentrations of 0.6 and 1.0 M, overneutralization is observed, and the coefficient C of eq 6 becomes negative.

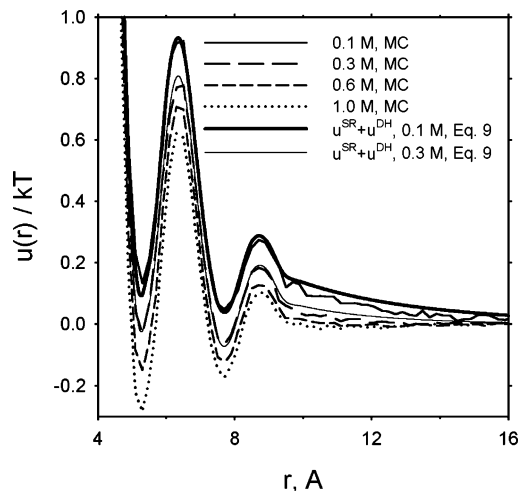


Figure 7. Cl^- – Cl^- PMFs obtained from MC simulations of MgCl_2 solutions at electrolyte concentrations of 0.1, 0.3, 0.6, and 1.0 M. Notations as in Figure 5. Parameter a_{ClCl} is set to 3.5 and 5.0 Å at concentrations of 0.1 and 0.3 M, respectively. At concentrations of 0.6 and 1.0 M, overneutralization is observed, and the coefficient C of eq 6 becomes negative.

approximation is correct only at $c = 0.1$ M, where all results (i.e., experiment, MC simulations, and eq 11) coincide. It is, in general, expected from Figures 5–7. At higher concentrations of electrolyte, a growing deviation between MC-simulated and theoretical results is observed, reaching about 0.8 kT at 1 M concentration (Figure 8). It notably exceeds model errors of MC-simulated $\ln \gamma$ (about 0.2 at $c = 1$ M, paper 1) and, therefore, cannot be ignored. This difference can be referred to the effect of interionic correlations. The last follows from the fact that parameters of mean-field approximation (eq 9) are obtained at an electrolyte concentration of 0.1 M, where interionic correlation effects are expected to be weak. The dependence of the solution permittivity on ionic concentration (eq 1) was also applied to MC simulations and eq 11. Values δ_i from eq 1 were set to $\delta_{\text{Mg}} = 24$ M^{-1} , $\delta_{\text{Ca}} = 23$ M^{-1} (ref 23a), and $\delta_{\text{Cl}} = 2$ M^{-1} (ref 21). The obtained discrepancies between results for $\epsilon = 78.5$ and $\epsilon = \epsilon(c)$ are almost equal in both cases of MC simulations and calculations via eq 11. This can be explained by the fact that the major part of the electrostatic component of

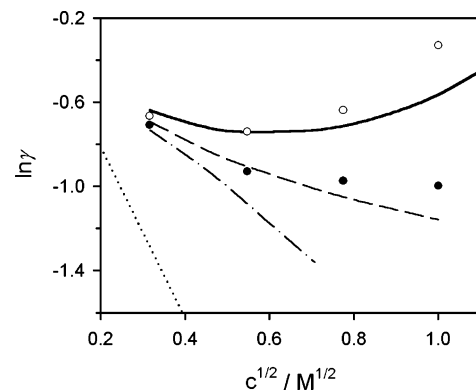


Figure 8. MgCl_2 activity coefficient calculations based on the effective ion–ion potentials reported in paper 1. Open circles are results of MC simulations of solutions of MgCl_2 at constant dielectric constant of solvent, $\epsilon = 78.5$. Filled circles are the same results at $\epsilon = \epsilon(c)$ via eq 1. Values of δ_i from eq 1 are given in the text. The dashed line is results of the activity coefficient calculations via eq 11 at $\epsilon = 78.5$. The dash–dotted line represents the same calculations at $\epsilon = \epsilon(c)$. The thick solid curve is experimental data for MgCl_2 . The dotted line is the DH limiting law.

the ion excess chemical potential is determined by the mean field at all concentrations studied. One can also see from Figure 8 that an impact of the ion hydration shell polarization on the activities is of the same magnitude but of opposite sign than the effect of interionic correlations.

Approximate Model of Ions

Equation 11 can be applied to formulation of a simplified implicit-solvent model of ions with hydration shell polarization. Such a model describes ions as hard-core interacting spheres bearing point charges in their centers. The hard-core interaction distances a_{ij}^{HC} are deduced from the effective interionic potentials. In general, these distances are nonadditive (Table 1). Like the PPM, the Coulomb interaction is supplemented by additional energy $\alpha_i E^2$ of the hydration shell polarization of ion i .

One can write the excess chemical potential μ_i of a real ion as

$$\mu_i = \mu_i^0 + (\mu_i - \mu_i^0) \quad (12)$$

where μ_i^0 is the excess chemical potential of an ion of species i obtained for the Coulomb, hard-core, and $\alpha_i E^2$ polarization interactions.

Because one can neglect all triple correlations for short-range interactions, parameters of the simplified model can be adjusted in such a way that the chemical potential μ_i^0 will include all (or almost all) free energy of the ion due to the mean electrical field and the formal polarization energy $\alpha_i E_j^2 + \alpha_j E_i^2$ of the ion hydration shell. Then the residue $(\mu_i - \mu_i^0)$ appears due to the difference between the true short-range part of the interionic potentials u_{ij}^{SR} and the formal polarization energy. As this difference is a short-range (i.e., pair-potential) effect, it will be expressed as $\mu_i - \mu_i^0 = \sum B_{ij} c_j$, where factors B_{ij} should not depend on ion concentrations c_j and the excess chemical potential of an ion will be written as

$$\mu_i = \mu_i^0 + \sum B_{ij} c_j \quad (13)$$

In other words, the model represents hypothetical electrolyte where ions are polarizable hard spheres immersed into a dielectric continuum of permittivity ϵ of pure solvent. At a contact of ions i and j , they possess nonadditive hard-core

TABLE 2: Linear Contributions $B_{ij}^0 c_j$ to the Ion Chemical Potentials for the Model of Polarizable Ions of True Hard-Core Diameters a_{ij}^{HC} (infinity dilution)

electrolyte	B_{11}^0 (kT/M)	B_{12}^0 (kT/M)	B_{22}^0 (kT/M)
NaCl	-0.11	0.14	0.00
KCl	-0.13	-0.11	0.00
MgCl ₂	0.00	-3.66	0.00
CaCl ₂	0.00	-5.80	0.00

TABLE 3: Ion Chemical Potential Parameters Calculated for Eqs 13 and 15 at Different Concentrations of Electrolyte

electrolyte	c (M)	a_{ij}^{HC} (Å)	B_{11} (kT/M)	B_{12} (kT/M)	B_{22} (kT/M)	$B^{\text{HC } a}$ (kT/M)
NaCl	0.1	4.5	-0.13	-0.49	0.02	0.46
	0.3	4.5	-0.13	-0.42	0.02	0.46
	0.7	4.5	-0.12	-0.40	0.02	0.46
	1.0	4.5	-0.12	-0.39	0.02	0.46
KCl	0.1	4.5	-0.16	-0.66	0.02	0.46
	0.3	4.5	-0.17	-0.58	0.02	0.46
	0.7	4.5	-0.17	-0.53	0.02	0.46
	1.0	4.5	-0.17	-0.51	0.02	0.46
MgCl ₂	0.1	7.0	0.18	-3.13	0.10	2.60
CaCl ₂	0.1	6.0	-0.09	-2.45	0.14	1.63

^a Contribution due to the “exclusion volume” term of eq 15 per electrolyte concentration.

diameters a_{ij}^{HC} , and the ion chemical potential includes a linear dependence on the local ionic concentrations.

One can easily determine coefficients B_{ij}^0 at infinity dilution of electrolyte solution. According to eq 11,

$$\beta\mu_i \xrightarrow{n_j^0 \rightarrow 0} \beta \sum_j n_j^0 4\pi \int_0^\infty dr r^2 \left(u_{ij}^{\text{SR}}(r) + \frac{q_i q_j}{\epsilon r} \right) \times \int_0^1 d\lambda \exp \left(-\beta \lambda \left(u_{ij}^{\text{SR}}(r) + \frac{q_i q_j}{\epsilon r} \right) \right) = \sum_j n_j^0 \frac{4}{3} \pi (a_{ij}^{\text{HC}})^3 + \sum_j n_j^0 4\pi \int_{a_{ij}^{\text{HC}}}^\infty dr r^2 \left(1 - \exp \left(-\beta \left(u_{ij}^{\text{SR}}(r) + \frac{q_i q_j}{\epsilon r} \right) \right) \right)$$

and, similarly,

$$\beta\mu_i^0 = \sum_j n_j^0 \frac{4}{3} \pi (a_{ij}^{\text{HC}})^3 + \sum_j n_j^0 4\pi \int_{a_{ij}^{\text{HC}}}^\infty dr r^2 \left(1 - \exp \left(-\beta \left(\frac{\alpha_i q_j^2 + \alpha_j q_i^2}{\epsilon^2 r^4} + \frac{q_i q_j}{\epsilon r} \right) \right) \right)$$

where a_{ij}^{HC} is the hard-core interaction distance between ions i and j . Then substitution of these expressions of μ_i and μ_i^0 into eq 12 leads to estimation of the coefficients B_{ij}^0 in eq 13:

$$\beta B_{ij}^0 = \frac{N_A}{1000} 4\pi \int_{a_{ij}^{\text{HC}}}^{R_{ij}^*} dr r^2 \exp \left(-\beta \frac{q_i q_j}{\epsilon r} \right) \times \left[\exp \left(-\beta \frac{\alpha_i q_j^2 + \alpha_j q_i^2}{\epsilon^2 r^4} \right) - \exp(-\beta u_{ij}^{\text{SR}}(r)) \right] \quad (14)$$

where R_{ij}^* is the minimal separation where u_{ij}^{SR} actually becomes $\alpha_i E_j^2 + \alpha_j E_i^2$.

Monovalent Cations. Parameters a_{ij} and a_{ij}^{HC} are given in Table 1. Parameters a_{ij}^{HC} are estimated from the effective interionic potentials (Table 3 of paper 1). The value of R_{ij}^* was set to 10 Å. The resulting coefficients B_{ij}^0 for NaCl and KCl

are given in Table 2. As seen from these data, magnitudes of B_{ij}^0 are low and do not exceed 0.15 kT/M. It confirms the previously known conclusion that the PM can well approximate the excess chemical potential of monovalent ions.¹⁰

Divalent Cations. Parameters a_{ij} and a_{ij}^{HC} for MgCl₂ and CaCl₂ are given in Table 1. The coefficients B_{ij}^0 from eq 14 are given in Table 2. The coefficient B_{11}^0 appears to be very low because of the damping factor $\exp(-\beta Z^2 e^2 / 4\pi \epsilon \epsilon_0 r)$ in eq 14 and small difference between u_{11}^{SR} and $2\alpha_1 E^2$ at $r > a_{ij}^{\text{HC}}$ (see, e.g., Figure 8 of paper 1). The magnitude of B_{12}^0 is very high and reaches a few kT per mole. This actually prevents applying the PM to divalent ions when their hard-core interaction distances are set to the true values.

Approximating Expression of the Ion Chemical Potential

We cannot write an explicit expression of μ_i^0 in eq 12 at finite concentration of ions. The dependencies $\mu_i^0(c)$ and $B_{ij}(c)$ on the ionic concentration in eq 13 should be obtained from MC simulations of polarizable ions with the hard-core contact distances a_{ij}^{HC} and polarizabilities α_i . However, at low ionic concentration, one can neglect interionic correlation effects and reduce the excess chemical potential of such idealized ions to a mean-field approximation like was done in eqs 9 and 11. Using this approximation of $\mu_i^0(c)$ and, on the other hand, eq 11 written for real u_{ij}^{SR} , it is possible to obtain factors $B_{ij}(c)$ in eq 13 for the ion excess chemical potential $\mu_i(c)$.

A mean-field approximation of μ_i^0 was used in MPB applications^{21,30} with the dependence of the local permittivity $\epsilon(r)$ of the electrolyte on ionic concentrations and external electric field E : $\epsilon(r) = \epsilon(r, c_1, c_2, E)$. In that approximation, all ions had the same hard-core diameter a^{HC} , and we will retain this simplification in the present study to see its impact on B_{ij} . The ion chemical potential μ_i^0 was calculated as if an ion i was gradually charged in the solvent of permittivity $\epsilon(c, E)$ and in the presence of pointlike other ions. The polarization of the ion hydration shell was referred only to the external field. On neglecting the local change of $\epsilon(c)$ due to the local variation of ionic concentrations around the ion, the excess chemical potential μ_i^0 in that approximation is expressed as

$$\mu_i^0 \approx \frac{4}{3} \pi (a^{\text{HC}})^3 kT \sum_j n_j^0 - \frac{q_i^2}{2\epsilon(c)} \frac{\kappa(c)}{1 + \kappa(c)a^{\text{HC}}} + \frac{q_i^2}{2a_i^\epsilon} \left(\frac{1}{\epsilon(c)} - \frac{1}{\epsilon} \right) \quad (15)$$

where $\epsilon(c)$ obeys eq 1, $\kappa(c)$ is the inverse DH length calculated with $\epsilon(c)$, a^{HC} the common hard-core diameter referred to all ions, and a_i^ϵ the radius of the dielectric sphere approximating the ion hydration shell (about 4 Å).²¹ The first term is the volume exclusion term, i.e., the work against the osmotic pressure of ionic gas. The second negative term is the DH chemical potential calculated with $\epsilon(c)$ instead of ϵ . The third term is the Born energy due to decrease of permittivity.

To derive an explicit expression of $\mu_i(c)$ according to eqs 11 and 13, eq 15 will be used as a definition of μ_i^0 . The second term of eq 15 can be expressed as

$$-\frac{q_i^2}{2\epsilon(c)} \frac{\kappa(c)}{1 + \kappa(c)a} \approx \sum_j n_j^0 4\pi \int_a^\infty dr r^2 \frac{q_i q_j}{\epsilon(c)r} \times \int_0^1 d\lambda \exp(-\lambda \beta W_{ij}(r)) \quad (16a)$$

where $W_{ij}(r) \approx q_j \psi_i(r)$ and

$$\psi_i(r) = \frac{q_i}{\epsilon(c)(1 + \kappa(c)a)} \frac{\exp(-\kappa(c)(r - a))}{r}$$

By using eqs 1 and 2, the third term of the expression of μ_i^0 is also written as a linear combination of concentrations:

$$\frac{q_i^2}{2a_i^\epsilon} \left(\frac{1}{\epsilon(c)} - \frac{1}{\epsilon} \right) \approx \frac{q_i^2}{\epsilon^2 a_i^\epsilon} \sum_j 4\pi\alpha_j n_j^0 \quad (16b)$$

However, the very presence of this third term of μ_i^0 is questionable even at moderate concentrations of ions. This term appears if one substitutes the effective potential $q_i q_j / (\epsilon(c)r) + \alpha_j 2\lambda (q_j / (\epsilon r^2))^2$ in eq 16a instead of $q_i q_j / (\epsilon(c)r)$. The factor 2λ reflects the quadratic dependence of this part of the effective potential on the coupling parameter λ , and we take into account that, even for 2:1 electrolyte solutions, $\exp(-\beta W_{ij}(r)) \approx 1$ at $r > 8$ Å and $c > 0.5$ M. As follows from this substitution, polarization of the ion i is excluded from the third term of eq 15, and only polarization energy $\alpha_j E_i^2$ of the hydration shell of ion j in the field of the ion i is considered. On the contrary, screening of this polarization potential is not taken into consideration at all, and such a substitution of the polarization energy of the ion j in eq 16a can only be done at infinity dilution. At finite concentrations of ions, the induced polarization energy is not a pairwise potential yet.

Expansions (eqs 16a,b) allow us to extract coefficients B_{ij} in eq 13 at finite electrolyte concentrations by using eq 11 (with $\epsilon(c)$ and $\kappa(c)$) and eq 15.

Equation 13 can be applied to derive an approximation of the chemical potential of a single ion in the strong external field. Such an approximation can be incorporated into advanced statistical mechanical theories such as the MPB theory³¹ to study ion distributions around highly charged biological macromolecules. By following the Kirkwood hierarchy of distribution functions,^{30,32} the excess part of the chemical potential of an ion near a macromolecule can be approximated as

$$\mu_i(r) \approx U_i^{\text{ext}}(r) + Z_i e \psi(r) + kT \int_{\text{SHC}} \sum_j n_j(r) \, \mathbf{dr} + \eta_i^0(r) + Z_i e \int_0^1 d\lambda \eta_i(r, \lambda) + \sum_j B_{ij} n_j(r) \quad (17)$$

where U_i^{ext} is the short-range PMF acting between the ion and atomic group of the macromolecule, $\psi(r)$ the mean electrostatic potential, $\eta_i^0(r)$ a work against electric forces minus forces acting on the ion charge at a transfer of ion i to point \mathbf{r} (at low ionic concentration $\eta_i^0(r) \approx \alpha_i (\nabla \psi(r))^2$),

$$\eta_i(r_1, \lambda) = \lim_{r_2 \rightarrow r_1} \left(\phi_i(r_1, r_2, \lambda) - \frac{\lambda q_i}{\epsilon_i r_{12}} \right)$$

and $\phi_i(r_1, r_2, \lambda)$ is the fluctuation potential of the ion of species i fixed at point r_1 , i.e., the difference between the mean potential $\psi_i(r_1, r_2)$ in the presence of the fixed ion i and the mean potential $\psi(r_2)$; the charge of the fixed ion is multiplied by the coupling parameter λ ; ϵ_i is the low dielectric constant of the ion spherical cavity approximating the ion hydration cluster of water molecules.

If eq 17 is applied with the linearized Loeb's closure,^{30,32} it is reduced to eq 15 in the case of bulk electrolyte. Then the first two and fourth terms of expression (eq 17) disappear. The third term becomes the first term in eq 15. The fluctuation

potential term corresponds to the second and third terms in eq 15. The rest $\sum B_{ij} n_j$ is a correction to the real excess chemical potential of ions according to eq 13. One may assume that coefficients B_{ij} remain the same as in the bulk because they reflect effects of the short-range interactions and mean-field approximation.

Monovalent Electrolytes. For NaCl and KCl, parameter a^{HC} was arbitrarily chosen somewhere between the maximal and minimal values of a_{ij} . Values of a_{ij} and a^{HC} are given in Tables 1 and 3. As was applied above, $\epsilon(c) = \epsilon = 78.5$ for 1:1 electrolytes. That is, μ_i^0 can be reduced to the DH excess chemical potential of PM ions in this case. Calculated values of B_{ij} for NaCl and KCl are given in Table 3. Coefficients B_{11} from Table 3 are close to values of B_{11}^0 from Table 2. Too negative coefficient B_{12} in comparison with B_{12}^0 reflects a rather negative value of the effective potential $u_{\text{NaCl}}^{\text{HC}}$ between the true hard-core distance $a_{\text{NaCl}}^{\text{HC}}$ (2.7 Å, Table 1) and the "mean" ion diameter a^{HC} in eq 15 (4.5 Å). It is clearly seen in Figure 3 of paper 1. This effect is even more pronounced for KCl. Coefficients B_{ij} weakly depend on the concentration of ions. It might suggest that coefficients B_{ij}^0 of the more refined model with ion diameters a_{ij}^{HC} are not changed too much at finite ion concentrations.

As follows from Table 3, activity coefficients of chlorides of alkali metals can be approximated by an expression assuming a model of about 4–5 Å diameter ions of equal sizes. Effects of dielectric saturation of the ion hydration shells can be neglected. At $c < 1$ M, the major part of the excess chemical potential of these ions can be described by the mean-field approximation, leading to a DH-like dependence (15) on electrolyte concentration. Interionic correlation effects can be neglected. The rest of the chemical potential is a linear function on anion and cation concentrations. Constant coefficients of this linear form reflect the difference between the real ion–ion PMF and the ion–ion PMF described in eq 15.

This linear correction is not low and consists from 0.1 to 0.6 kT/M for a particular species ion concentration. As follows from comparison of Tables 2 and 3, a significant part of the coefficients B_{ij} originates from the difference of the true mean field of the ion and the mean field described in eq 15 (eq 16a). When the hard-core contact distances are set close to the values a_{ij}^{HC} (i.e., we refer μ_i^0 to a model of ions of variable size a_{ij}^{HC}), the additional linear correction $\sum B_{ij}^0 c_j$ of the ion activity coefficient appears to be notably lower.

Divalent Cations. Parameters of eqs 13 and 15 are given in Tables 1 and 3. The coefficients B_{ij} were obtained via eqs 11, 13, and 15–16 at neglecting the long-range asymptotes $\alpha_j E_j^2 + \alpha_j E_i^2$ of u_{ij}^{SR} and omitting the third term in eq 15, as this part of the ion–ion interaction potential is assumed to be screened at finite concentration of ions. However, $\epsilon(c)$ and $\kappa(c)$ dependencies were applied. Values δ_i from eq 1 are given above. Coefficients B_{ij} are given in Table 3. To diminish the contribution of the mean-field deviation to coefficients B_{11} , the parameter a^{HC} of the model was set equal to value of the a_{11} parameter. It was taken 7 Å for MgCl_2 and 6 Å for CaCl_2 .

Conclusions

In this second study of effective interionic potentials, the excess chemical potential of a hydrated ion was expressed in an explicit form by using these effective potentials. Invoking auxiliary arguments, an ion model approximating the ion chemical potential was explored. It was shown that application of approximation 9 to eq 10 of statistical mechanics allowed us to reproduce electrolyte activity coefficients obtained from

MC simulations with the effective ion–ion potentials. This reproduction is successful for up to 1 M concentration of alkali metal chloride solutions and for up to 0.1 M solutions of alkaline earth metal chlorides. This range corresponds to electrolyte concentrations at which MC simulations with the effective ion–ion potentials successfully reproduce experimental activity coefficients.

The reproduction of simulated and experimental activities by application of eq 11 is based on approximation 9 of the ion pair correlation functions. Equation 9 is a mean-field approximation that does not take into consideration the interionic correlations for long-range Coulomb electrostatics and treats the non-Coulombic part of ion–ion interaction as a pair potential. Therefore, one conclusion is that the interionic correlations and three-particle effects on non-Coulombic interactions play only a minor role in the ion free energy of 1:1 electrolytes at concentrations up to 1 M and 2:1 electrolytes at concentrations up to 0.1 M.

The role of interionic correlations appears only at moderate to high concentrations of 2:1 electrolytes as follows from comparison of MC-simulated activity coefficients with results from eq 11 (Figure 8). In real 2:1 electrolytes, this effect has to be diminished by polarization effects and affected by three-particle short-range interactions. The effect of polarization deficiency of the saturated ion hydration shell on activity coefficients of MgCl_2 appears to be of the same magnitude but of opposite sign than the effect of interionic correlations. It is clearly seen from a comparison of results at $\epsilon = 78.5$ and $\epsilon = \epsilon(c)$ shown in Figure 8.

The second conclusion concerns applicability of the primitive model. Term $\sum B_{ij}^0 c_j$ in eq 13 is a difference of the excess chemical potential of real ions and the excess chemical potential of PM-like ions with the true hard-core contact distances a_{ij}^{HC} . For monovalent electrolytes, magnitudes of B_{ij}^0 are low, which allows us to approximate electrolyte properties by the PM with adjusted hard-core diameters of ions.^{10,16,26} For divalent electrolytes, values of B_{12} reach a few kT per mole, which does not allow us to apply the PM with hard-core interaction distances chosen close to real ones. Successful application of the PM to 2:1 electrolyte solution can be reached by fitting diameters of hydrated ions¹⁶ that appear to be notably different from the true a_{ij}^{HC} (Table 1). Besides, in real interionic PMFs, a_{12}^{HC} is not equal to $(a_{11}^{\text{HC}} + a_{22}^{\text{HC}})/2$, and the polarization deficiency effects of the ion hydration shells cannot be neglected in 2:1 electrolytes at $c > 0.1$ M.

To describe divalent cations, an attempt to improve an approximate model of ions has been made in the present study. This is a development of the primitive polarization model discussed in ref 21. In the PPM, a simple approximation of the ion hydration shell was represented by a low-polarizable

dielectric sphere of radius a_i^{ϵ} and permittivity ϵ_i . The approximate polarization model retains these parameters, along with three parameters a_{ij}^{HC} (or one common parameter a^{HC}) treated as hard-core interaction diameters. Now the chemical potential of a single ion i is endowed with coefficients B_{ij} , reflecting all the rest of the ion free energy $\sum B_{ij} c_j$ linearly depending on the local concentrations of anions and cations. Such a model can be applied in iterative MC simulations of electrical double layers around highly charged biological macromolecules. With approximate expression (eq 17) of the ion chemical potential, it can be used in MPB calculations for such systems.

References and Notes

- (1) Gavryushov, S.; Linse, P. *J. Phys. Chem. B*, **2006**, *110*, 10878.
- (2) Berendsen, H. J. C.; Grigera, J. R.; Straatsma, T. P. *J. Phys. Chem.* **1987**, *91*, 6269.
- (3) Åqvist, J. *J. Phys. Chem.* **1990**, *94*, 8021.
- (4) Smith, D. E.; Dang, L. X. *J. Chem. Phys.* **1994**, *100*, 3757.
- (5) Dang, L. X. *J. Am. Chem. Soc.* **1995**, *117*, 6954.
- (6) Dang, L. X. *J. Chem. Phys.* **1992**, *96*, 6970.
- (7) (a) Rasaiah, J. C.; Friedman, H. L. *J. Chem. Phys.* **1969**, *50*, 3965. (b) Rasaiah, J. C.; Card, D. N.; Valleau, J. P. *J. Chem. Phys.* **1972**, *56*, 248.
- (8) Waisman, E.; Lebowitz, J. L. *J. Chem. Phys.* **1972**, *56*, 3086.
- (9) (a) Blum, L. *J. Mol. Phys.* **1975**, *30*, 1529. (b) Blum, L.; Høye, J. S. *J. Phys. Chem.* **1977**, *81*, 1311.
- (10) Sloth, P.; Sørensen, T. S. *J. Phys. Chem.* **1990**, *94*, 2116.
- (11) (a) Outhwaite, C. W. *J. Chem. Phys.* **1969**, *50*, 2277. (b) Outhwaite, C. W. *J. Chem. Soc., Faraday Trans. 2* **1987**, *83*, 949.
- (12) (a) Andersen, H. C.; Chandler, D. *J. Chem. Phys.* **1970**, *53*, 547. (b) Andersen, H. C.; Chandler, D. *J. Chem. Phys.* **1972**, *57*, 1918.
- (13) (a) Pitzer, K. S. *J. Phys. Chem.* **1973**, *77*, 268. (b) Pitzer, K. S.; Mayorga, G. *J. Phys. Chem.* **1973**, *77*, 2300.
- (14) Kjellander, R. *J. Phys. Chem.* **1995**, *99*, 10392.
- (15) Nordholm, S. *Aust. J. Chem.* **1984**, *37*, 1.
- (16) Abbas, Z.; Gunnarsson, M.; Ahlberg, E.; Nordholm, S. *J. Phys. Chem. B* **2002**, *106*, 1403.
- (17) Card, D. N.; Valleau, J. P. *J. Chem. Phys.* **1970**, *52*, 6232.
- (18) Valleau, J. P.; Cohen, L. K.; Card, D. N. *J. Chem. Phys.* **1980**, *72*, 5942.
- (19) Abramo, M. C.; Caccamo, C.; Malescio, G.; Pizzimenti, G.; Rogde, S. A. *J. Chem. Phys.* **1984**, *80*, 4396.
- (20) Lyubartsev, A. P.; Laaksonen, A. *J. Chem. Phys.* **1999**, *111*, 11207.
- (21) Gavryushov, S.; Linse, P. *J. Phys. Chem. B* **2003**, *107*, 7135.
- (22) Hückel, E. *Phys. Z.* **1925**, *26*, 93.
- (23) (a) Hasted, J. B.; Ritson, D. M.; Collie, C. H. *J. Chem. Phys.* **1948**, *16*, 1. (b) Buchner, R.; Hefter, G. T.; May, P. M.; *J. Phys. Chem. A* **1999**, *103*, 1.
- (24) Chandra, A. *J. Chem. Phys.* **2000**, *113*, 903.
- (25) Zasetky, A. Yu.; Svishchev, I. M. *J. Chem. Phys.* **2001**, *115*, 1148.
- (26) Fawcett, W. R.; Tikanen, A. C. *J. Phys. Chem.* **1996**, *100*, 4251.
- (27) Electrostatic system units are used in all following equations.
- (28) Hill, T. L. In *Statistical Mechanics*; McGraw-Hill: New York, 1956.
- (29) Robinson, R. A.; Stokes, R. H. *J. Am. Chem. Soc.* **1948**, *70*, 1870.
- (30) Gavryushov, S.; Zielenkiewicz, P. *J. Phys. Chem. B* **1999**, *103*, 5860.
- (31) Gavryushov, S.; Zielenkiewicz, P. *Biophys. J.* **1998**, *75*, 2732.
- (32) Carnie, S. L.; Torrie, G. M. *Adv. Chem. Phys.* **1984**, *56*, 141.